



HAL
open science

Hybrid cooling based battery thermal management using composite phase change materials and forced convection

Mohamed Moussa El Idi, Mustapha Karkri, Mahamadou Abdou Tankari,
Stéphane Vincent

► To cite this version:

Mohamed Moussa El Idi, Mustapha Karkri, Mahamadou Abdou Tankari, Stéphane Vincent. Hybrid cooling based battery thermal management using composite phase change materials and forced convection. *Journal of Energy Storage*, 2021, 41, pp.102946. 10.1016/j.est.2021.102946 . hal-04316619

HAL Id: hal-04316619

<https://hal.u-pec.fr/hal-04316619>

Submitted on 22 Jul 2024

HAL is a multi-disciplinary open access archive for the deposit and dissemination of scientific research documents, whether they are published or not. The documents may come from teaching and research institutions in France or abroad, or from public or private research centers.

L'archive ouverte pluridisciplinaire **HAL**, est destinée au dépôt et à la diffusion de documents scientifiques de niveau recherche, publiés ou non, émanant des établissements d'enseignement et de recherche français ou étrangers, des laboratoires publics ou privés.



Distributed under a Creative Commons Attribution - NonCommercial 4.0 International License

Hybrid cooling based battery thermal management using composite phase change materials and forced convection

Mohamed Moussa EL IDI^{1,2*}, Mustapha KARKRI¹, Mahamadou ABDOU TANKARI¹, Stéphane VINCENT²

¹Université Paris- Est, CERTES, 61 Av. du Général de Gaulle, 94010 Créteil Cedex, France.

²Université Gustave- Eiffel, Laboratoire MSME UMR CNRS 8208, Université Paris-Est Marne-La-Vallée, Marne-La-Valle F-77454, France

*Corresponding author: moussa.elidi@gmail.com

Abstract: *This paper investigates the thermal management performance of a novel system using phase change material (PCM) composite for Lithium-ion battery in cell scale. An experimental platform was developed to study thermal phenomena in Li-ion cell. The system was designed on the basis of heat flux measurements. The cells are embedded in a PCM composite material. The assembly is lodged in an aluminum mold manufactured by 3D printing. The impact of the addition of metal foam and forced convection was evaluated. The results showed that the proposed system allows to keep the temperature of Li-ion cell around the optimal operating temperature, 25°C. It's also found that the addition of an aluminum foam allows a more efficient thermal management of the cell.*

Keywords: Phase change material (PCM), Battery Thermal Management System (BTMS), Metal foam, Li-ion

Nomenclature

C	Specific heat capacity, ($J \cdot kg^{-1} \cdot K^{-1}$)	T	Temperature, (K)
ρ	Density, ($kg \cdot m^{-3}$)	k	Thermal conductivity, ($W/m \cdot K$)
Q	Heat flux, (W)		
L_f	Latent heat of fusion ($J \cdot kg^{-1}$)		
t	Time, (s)		

1. Introduction:

One of the main objectives of the world's energy transition is to reduce the amount of CO₂ in the atmosphere. Currently, the global energy is dominated by fossil fuels by about 80% [1]. The transportation sector is among the largest consumers of fossil fuels [2]. One way to reduce carbon emissions in the transportation sector is to replace fossil fuel engines with electric vehicles (EVs) using clean energy sources or hybrid vehicles. Because of their high specific energy density, good stability and low density, Li-ion batteries are generally considered the first choice for EVs [3]. The development of EVs is certainly dependent on that of Li-ion batteries. During charge and discharge cycles, Li-ion batteries experience a rise in temperature, which appears to be the main cause of performance and battery life degradation. The study conducted by Waldmann et al. [4] showed that the high temperatures accelerate the cathode electrode degradation which leads to a decrease of the batteries capacity. This is an agreement with the study made by Ramadass et al [5]. It was found that the capacity of Sony 18650 cells decreases down to 70% after 500 cycles at higher temperatures. In addition to the temperature increasing, the non-uniformity of heat transfer between cells can cause negative effects on the overall performance of the battery. Thereby the development of efficient Li-ion Batteries Thermal Management System (BTMS) appears necessary to ensure better performance, autonomy and optimal lifespan.

The BTMS is currently categorized into three principal categories, active system, passive system, and hybrid system. Amongst them, active cooling systems by air or liquid are the most widely used. However, air systems have its cooling limitations due to its low heat capacity and thermal

44 conductivity. Liquid systems are costly in terms of energy consumption, investment and maintenance.
45 Passive systems are a less expensive alternative. Passive systems can be classified into two principal
46 groups: Heat pipes [6] and Phase Change Material (PCM) composites.

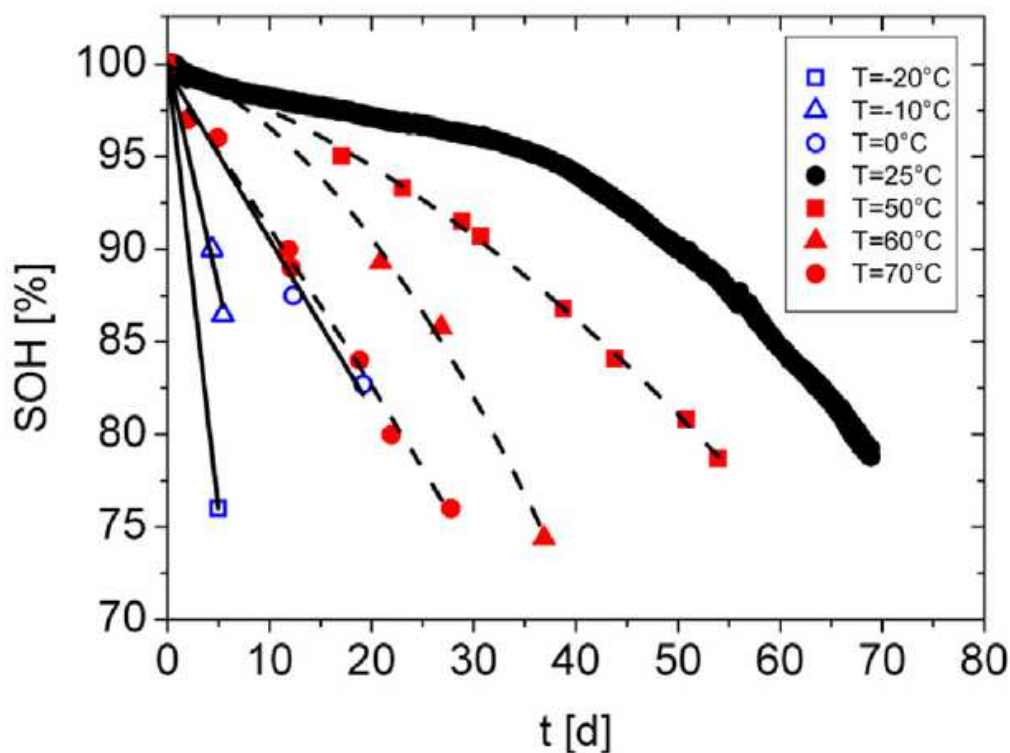
47 During the solidification and melting process of PCM, they can absorb and release latent heat
48 during the electrical charge and discharge cycles of batteries, while their temperature remains almost
49 constant. In the last two decades there has been a lot of interest in PCM and PCM composites systems
50 [7]. BTMS using PCM systems can present a problem of low thermal conductivity, regeneration or
51 leaks in the liquid state. The regeneration problem can be solved by the addition of an optimized and
52 intelligent active system that only triggers when needed to evacuate the heat stored in the PCM. PCM
53 low thermal conductivity can be improved by integrating a material with high thermal conductivity
54 [8] such as fins [9], porous-graphite [10], expanded graphite [11–13], nanoparticles [14], and high
55 porosity metal foam (MF) [15–20]. Among these solutions, MF have special properties that make them
56 a very good candidate to improve the thermal conductivity of a PCM [21]. MF are porous media with
57 large porosities and large contact areas per unit volume [22].

58 BTMS using PCM was proposed for the first time by Hallaj and Selman [7]. The authors compared
59 the efficiency of their proposed system with an air system. It was found that the use of PCM allows a
60 more efficient thermal management with a reduction of about 8°C compared to an air system. The use
61 of PCM can be particularly effective to control the temperature of Li-Ion batteries in high temperature
62 environments [23–25]. Wenga and his co-workers investigated the thermal performance of PCM and
63 branch-structured fins for cylindrical power battery in a high-temperature environment [23]. The
64 authors tested different PCM types with different phase change temperatures in a high-temperature
65 environment. It was found that the PCM with a phase change temperature of 46 °C offers the best
66 cooling effect at a high ambient temperature (40°C). In [24] the result showed that the use of PCM - fin
67 structure with optimized design allowed to keep the maximum temperature of the battery under 51°C
68 at high discharge rate of 3C and ambient temperature of 40°C. Ling et al. [26] conducted an
69 experimental and numerical study on the thermal management of a Li-ion battery by an expanded
70 paraffin-graphite composite. They tested paraffin with different melting temperatures (36°C, 44°C and
71 52°C). The cells were replaced by heating elements that simulate the same thermal behavior of the
72 cells. It was found that PCM composites with high or low phase change temperature are not suitable
73 for battery thermal management systems. Hussain et al. [27] utilized a graphene coated nickel foam
74 saturated with paraffin to study the performance of the thermal management system of Li-ion cell.
75 They compared the system with a system using nickel foam. They found that the cell surface
76 temperature is 17% less using graphene coated nickel foam saturated with PCM compared to using
77 nickel foam. Li et al. [28] conducted an experimental study on the thermal performance of BTMS
78 using a pure PCM and a PCM-MF composite. It was found that the use of PCM-Copper foam
79 composite leads to lower temperatures with a more uniform temperature field compared to pure
80 paraffin.

81 Recently, some efforts have been focused on the study of hybrid systems for the Li-ion batteries
82 thermal management by adding an active system in order to solve the problems of passive BTMS
83 using PCM composite [29–35]. However, most research has studied numerically this problem.
84 Mashayekhi et al. [34] proposed hybrid system. A paraffin RT44 incorporated in copper foam was
85 used as passive system. For active system the authors proposed an aluminum minichannel containing
86 coolant (Al₂O₃ nanofluid). The evaluation of the thermal performance of the proposed BTMS showed
87 that in high discharge rates passive system was inefficient to keep the battery temperature below the
88 safety limit (60 °C). It's was -also- found that the addition of nanofluid allows to reduce the maximum
89 temperature reached by batteries by 15.5% in active system case and 8.5% in hybrid system case.
90 Bamdezh and Molaieimesh [30] proposed a hybrid system by combined an air cooling system and a
91 PCM composite. The numerical results showed that the maximum temperature difference of the
92 studied battery was reduced. They do not exceed 1.5°C. Inspired by Tesla cooling system, Lv et al [35]

93 were proposed a novel BTMS using PCM coupled with forced air convection. It's was found that the
94 proposed system compared to passive system can reduce the used PCM composite weight by ~70%
95 and increasing the energy density of the battery module from 107.8 to 121.6 Wh kg⁻¹.

96 The majority of studies in the literature are numerical or experimental studies simplified by
97 replacing, for example, Li-ion cells with a heating element and focus on maintaining the temperature
98 of the batteries in a temperature range between 40°C and 60°C. However, the optimal temperature
99 range is between 15°C and 35°C [36]. Studies performed in [4] under a current of 1C have shown that
100 the operating temperature for optimal lifetime for 18650 Li-ion cells is 25°C. Below 25°C, the aging rate
101 increases with decreasing temperature, while above 25°C, aging is accelerated with increasing
102 temperature, Figure 1. In this paper we proposed a new BTMS using PCM-MF composite. The aim of
103 the proposed BTMS is to keep cell temperature around optimal temperature of 25°C under a 1C
104 charge/ discharge rate. An experimental platform will be presented and described. The mold
105 intended to house the cell and the PCM composite was manufactured by 3D metal printing. The heat
106 dissipated by the cell has been calculated from the experimental results and by used MATLAB code.
107 The results will be presented and discussed.



108
109 **Figure 1:** SOH curves measured as a function of time for cycles of 1 C at different temperatures [4].

110 **2. Materials and methods**

111 **2.1. Materials**

112 The selected PCM used in this work was paraffin RT27. The phase change temperature of the PCM
113 was around 27°C and specific density, 179 KJ/kg [37]. The metal foam consisted of an Aluminum
114 Foam (AF) with a porosity of 93%. The choice of this foam is the result of our previous work [17,18].
115 The incorporation of paraffin RT27 in AF was done following the protocol presented in [16]. DSC,
116 Hot- Disk, Transient Guarded Hot Plate Technique (TGHT) are used to characterize the used
117 materials [16,37]. The elaboration protocol and the experimental devices and characterization methods

118 are well described in our recently published article [16]. The proprieties of paraffin RT27 and paraffin
 119 RT27- AF composite used for the present study are given in **Table 1**.
 120

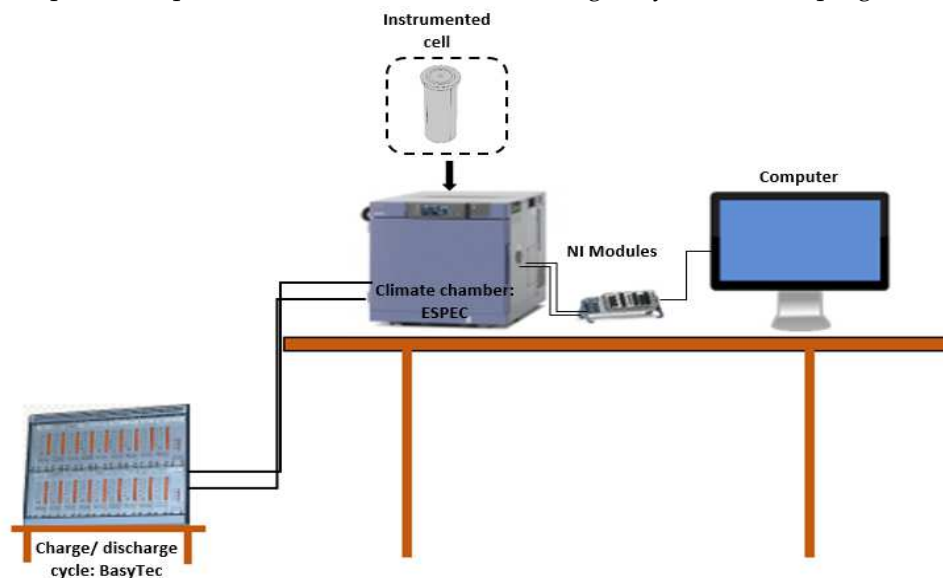
121 **Table 1:** Thermophysical properties of paraffin RT27, RT27- Metal foam and aluminum foam.

properties	Paraffin RT27	Aluminum	RT27- Metal foam composite
Density ($kg.m^{-3}$)	870	2800	1005
Heat capacity–solid ($J.K^{-1}.kg^{-1}$)	2400	910	1195.68
Latent heat ($KJ.kg^{-1}$)	179		
Melting temperature (K)	300.15		300.15
Dynamic viscosity ($Kg.m^{-1}.s^{-1}$)	3.42×10^{-3}		
Thermal conductivity –solid ($W.K^{-1}.m^{-1}$)	0.24	237	4.49
Density – liquid ($kg.m^{-3}$)	760		902
Heat capacity –liquid ($J.K^{-1}.kg^{-1}$)	1800		
Thermal conductivity – liquid ($W.K^{-1}.m^{-1}$)	0.15		
β (K^{-1})	0.5×10^{-3}		

122

123 2.2. Experimental platform

124 The experimental platform developed in this work to study thermal phenomena in Li-ion cell is
 125 shown in *Figure 2*. The cell is connected to BaSyTec system which ensures the battery charge/
 126 discharge. Commercially available 18650 Li-ion cell with a nominal capacity of 2500 mAh were
 127 purchased from VARTRA. The cathode and anode of the Li-ion cells were -respectively-
 128 LiNi0.5Co0.2Mn0.3O2 and graphite. Cell electrical and geometrical characteristics are provided by the
 129 manufacturer. *Figure 3 (a)* shows a picture of the cell used in the present study. It's a cylindrical with
 130 dimensions: d=18mm; H=65mm. Thermocouples type K connected to a NI data acquisition system to
 131 monitor the cell temperature. A cylindrical sensor encapsulates the cell to measure radial heat flux
 132 dissipated by the cell. The instrumented cell is placed in a ESPEC-642 climatic chamber provided by
 133 ES Equipements Scientifiques to control the ambient temperature and humidity. The studied cell is
 134 suspended in order to avoid thermal exchanges by conduction between the battery surface and the
 135 external environment, *Figure 3 (a)*. The climatic chamber is equipped with a fan which allows to keep
 136 a homogeneous temperature in the climatic chamber. This causes a weak forced convection in the case
 137 of a constant imposed temperature. All instruments are managed by a LabVIEW program.

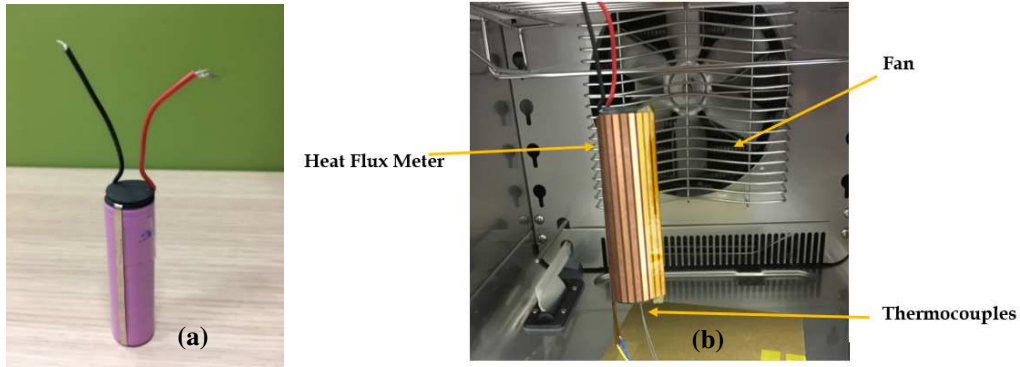


138

139

Figure 2: Experimental testbed

140



141

142

Figure 3: (a) Cell, (b) Instrumented cell in climatic chamber ESPEC-642

143

3. Results

144

3.1. Li-ion cell thermal behavior without BTMS

145

This work is part of the continuity of our recently published works [38]. In the present work we studied axial heat flux density and thermal properties of the cell using Hot-Disk.

146

147

The axial heat flux density is measured with a Captec Heat Flux Meter in the form of a disk with a diameter of 18.5mm and a thickness of 0.5mm, Figure 4. The disk is glued to the underside of the cell, Figure 5. Figure 11 displays a comparison between axial and radial heat flux density. The results show that the axial heat flux density is higher. Therefore, we can assume that Li-ion cells have higher axial thermal conductivity compared to radial thermal conductivity. To confirm this hypothesis, a characterization of the thermal conductivity of the cells has been carried out.

148

149

150

151

152

153

The thermal properties of the cell were determined using the Hot-Disk transient method [39,40]. The use of Hot-Disk for the thermal characterization of Li-ion batteries is described in [41]. Figure 7 shows the setup used to characterize the thermal properties of the cells. The measurements were repeated for ten times to ensure the accuracy and repeatability of the results. Table 2 summarizes the thermophysical properties of the batteries used in this study. It was found that the axial conductivity is 31.2 W/(m.K) and the radial conductivity is 0.2 W/(m.K).

154

155

156

157

158

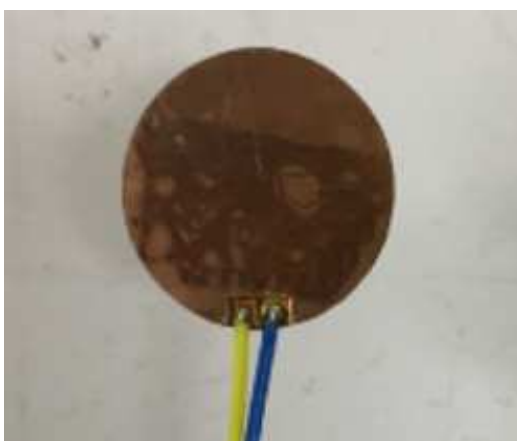


Figure 4 : Heat Flux Meter, disk

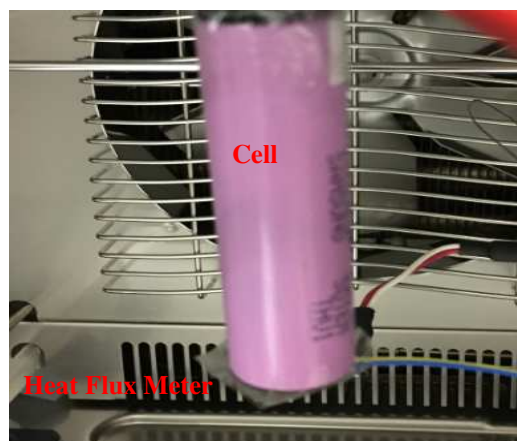
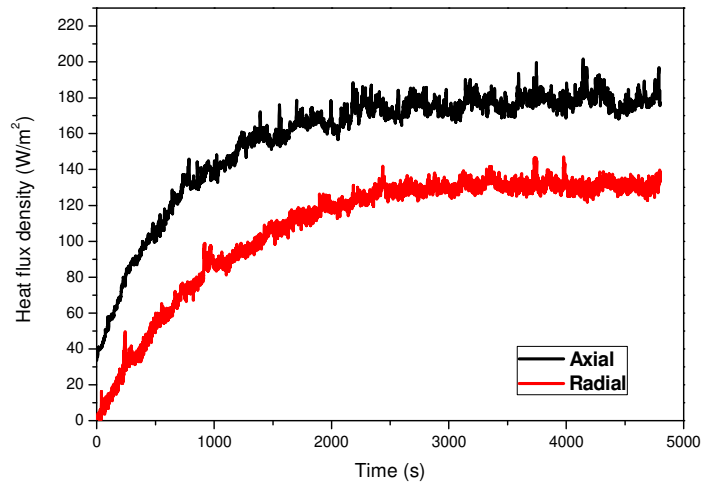


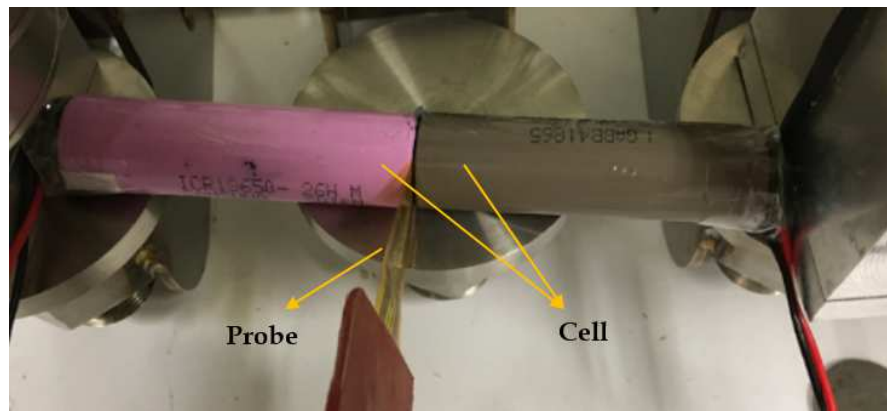
Figure 5 : Cell instrumented by Heat Flux Meter "disk"



159

160

Figure 6: Radial and axial heat flux density



161

162

Figure 7: Thermal characterization of the cells by Hot-Disk

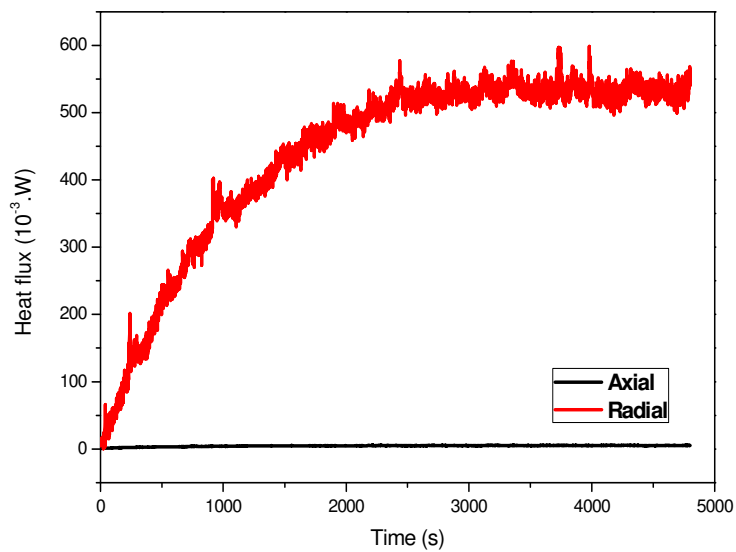
163

164

165

166

Figure 8 shows the temporal evolution of the radial heat flux versus axial heat flux. It can be seen that the axial flow is small compared to the radial flow. In fact, the axial flux represents about 0.9% and the radial flux 99.1%.



167

168

169

Figure 8: Radial and axial heat flux

170

Table 2: Thermophysical properties of the cell

	k , Axial	k , Radial	C_p	ρ
	$W.m^{-1}.K^{-1}$	$W.m^{-1}.K^{-1}$	$J.kg^{-1}.^{\circ}C^{-1}$	$Kg.m^{-3}$
Li-in Cell	31.15	0.2	1726	2700
Uncertainties	± 0.033	± 0.027	± 0.021	

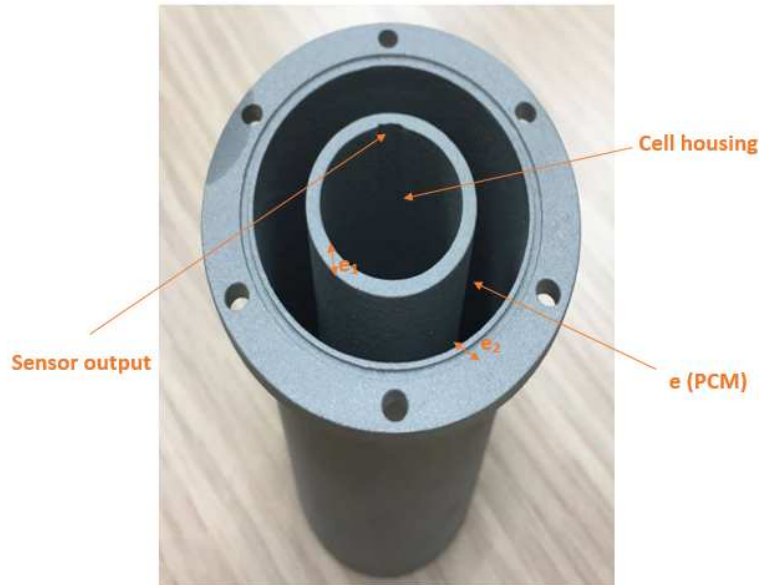
171

172

173 The approach we followed to size our system is well described in [38]. The results give a PCM
174 thickness of 2.8 mm. We approximate to 3 mm.

175 3.2. Li-ion cell thermal behavior with BTMS

176 The studied cell is placed in an aluminum mold. **Figure 9** shows a photograph of the mold used
177 with the details of its geometrical parameters. The mold takes the form of two hollow coaxial
178 aluminum cylinders, height h and thicknesses e , e_1 and e_2 . The inner cylinder has the same diameter as
179 the cell. A PCM composite is inserted between the two cylinders. A groove is provided at the internal
180 cell cylinder interface. It is used to accommodate the temperature sensors and the flowmeter cables.
181 The design of these molds takes into account the volume expansion of the PCM. Aluminum was
182 selected as an acceptable compromise between thermal properties, density and cost. The mold was
183 manufactured by high precision 3D metallic printing.

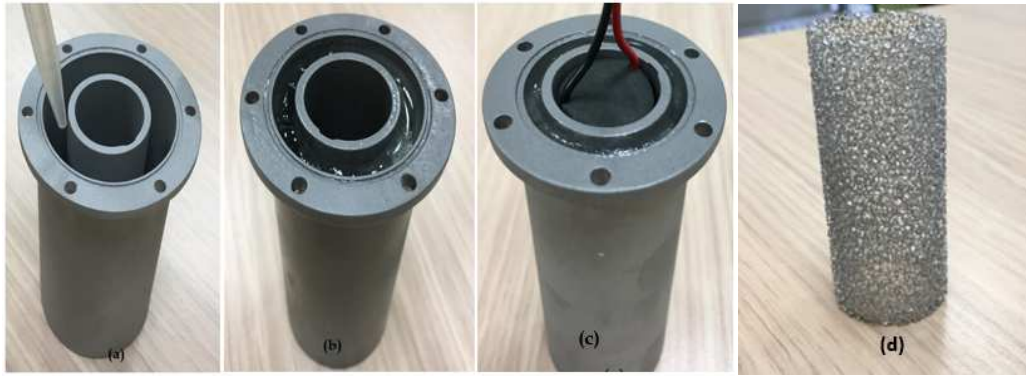


184

185

Figure 9: Aluminum mold used in this study

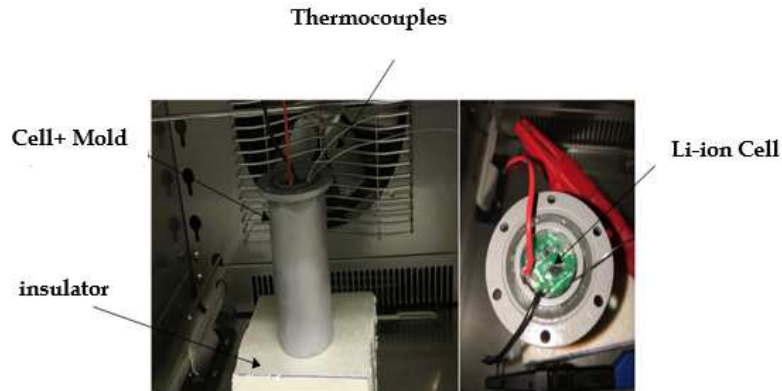
186 Liquid paraffin is injected into the vacuum designed to contain it. After filling, the whole unit is
187 cooled in the climatic chamber to an imposed temperature of 22°C. **Figure 10** (a) provides a
188 photograph during filling, **Figure 10** (b) is after filling and **Figure 10** (c) is after the integration of the
189 cell. Before inserting the cell into the mold, the protection of all connections is necessary to avoid any
190 direct contact between the aluminum mold and the cell connections.



191
192 **Figure 10:** *Experimental protocol*

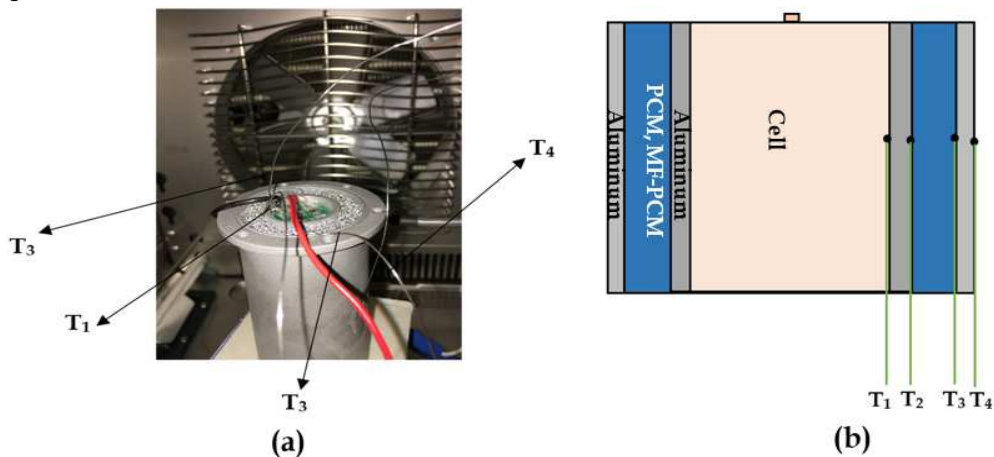
193 In the case of an MF-PCM composite, the metal foam is cut by a laser cutting system from the
194 EROSFER company in the form of tubes with dimension $h \times e$, **Figure 10** (d).

195 The instrumented cell is housed in the climatic chamber. The base of the mold is insulated by
196 expanded polystyrene, **Figure 11**.



197
198 **Figure 11:** *Cell housed in the climatic chamber*

199 In order to evaluate the thermal performance of the paraffin RT27 and paraffin RT27- AF
200 composite and their capacities to absorb the heat generated by the cell during successive
201 charge/discharge cycles, the evolution of the radial temperature was monitored at the interfaces
202 thanks to four K-type thermocouples: T_1 , T_2 , T_3 and T_4 . **Figure 12** (a) provides a photo illustrating the
203 location of the thermocouples and **Figure 12** (b) shows a schematic diagram of the location of the four
204 thermocouples.



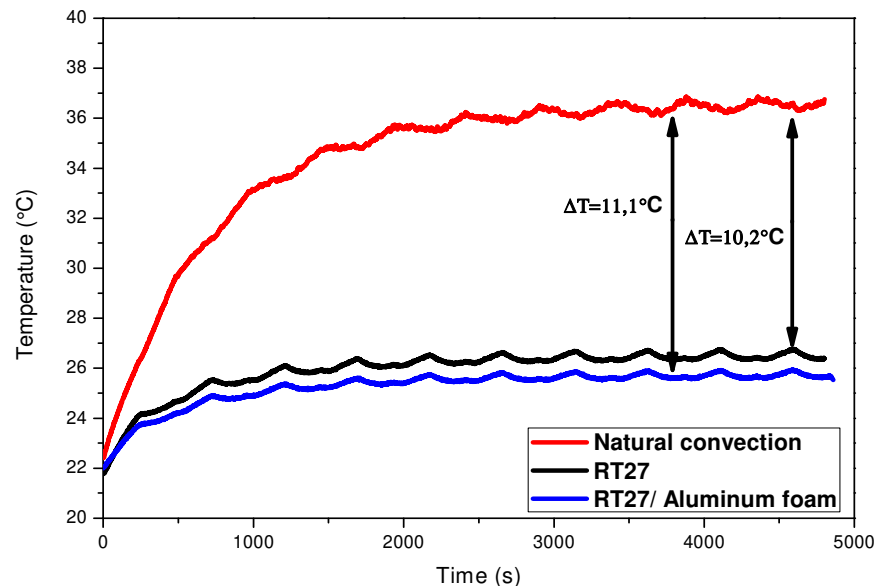
205
206 **Figure 12:** Thermocouple positions (a): Photo, (b): Schematic diagram

207 3.2.1. Impact of BTMS on cell temperature

208 **Figure 13** shows a comparison of temperature evolution measured by thermocouple T_1 as a
209 function of time. The results presented for the three cases studied include natural convection (cell
210 without proposed BTMS), paraffin RT27 and the AF (porosity 0.93, pore density 40PPI) - paraffin RT27
211 composite. The solicitation is a current of 1C (2.5A) for ten successive uninterrupted 8-minute
212 charge/discharge cycles. For thermal management with the pure paraffin RT27 and the Paraffin RT27-
213 AF composite, the imposed temperature is 22°C. Ventilation is active to promote heat exchange
214 between the evaporator (or condenser in the case of heating) and the air inside the climatic chamber.

215 The results show that the proposed BTMS (pure paraffin RT27/ paraffin RT27- AF composite) can
216 significantly reduce the temperature of the cell. The black and blue curves, respectively, show the
217 management of the time evolution of the cell temperature in the cases of pure paraffin RT27 and the
218 Paraffin RT27- AF composite. Both curves show that a steady state is reached after two cycles versus
219 five cycles in the case of natural convection. Comparing the steady state cell temperatures, we observe
220 that the cell temperature of the natural convection reached 36.7°C, while the pure paraffin RT27
221 reached 26.5°C and thermal management with the paraffin RT27- AF composite (0.93, 40PPI) reached
222 25.6°C. In conclusion, the pure paraffin RT27 allowed the cell temperature to reduce by 10.2°C
223 (average deviation in the steady state) and the paraffin RT27- AF (0.93, 40PPI) composite reduced by
224 11.2°C (average deviation in the steady state). The results show that the proposed system can maintain
225 the cell temperature very close to the optimal operating temperature of 25°C.

226 The comparison of the results of the present study with the studies done by [42–44] points to the
227 role of PCM phase changes temperature on the BTMS performance. In [42] the authors used a paraffin
228 wax with phase change temperature around 44°C. Experiments were carried out for the battery
229 contained in the housing for different heat exchange conditions, natural convection without PCM,
230 pure PCM, and composite PCM and fin structure. The result showed that the proposed system kept
231 the temperature around 55°C in the heat input of 6W case.



232
233 **Figure 13:** Measured temperature evolution with and without thermal management system

234 3.2.2. Temperature distribution without forced convection

235 In order to simulate a cell placed in a very confined area (battery pack of electric vehicle), tests
236 without forced convection are performed. The assembly is placed in the climatic chamber, initially at a
237 thermal equilibrium of 22°C, isolated from any heat exchange with the ambient environment.

238 **Figure 14**, and **15**, show – respectively- the temperature evolution in the case of pure paraffin RT27
239 and paraffin RT27- AF composite. The results show the total melting of the paraffin in both cases. This

240 corroborates the results of our previous numerical study presented in [38]. An underestimation of
 241 necessary PCM volume to absorb the heat generated by the cell leads to high temperatures. The
 242 results show that the addition of a MF significantly reduced the temperature difference between the
 243 cell and the MF-PCM composite due to the improvement of effective thermal conductivity of the MF-
 244 PCM composite. The temperature difference between T_1 and T_2 was 2.5°C in the case of pure paraffin
 245 RT27 and 1.6°C in the case of paraffin RT27- AF.

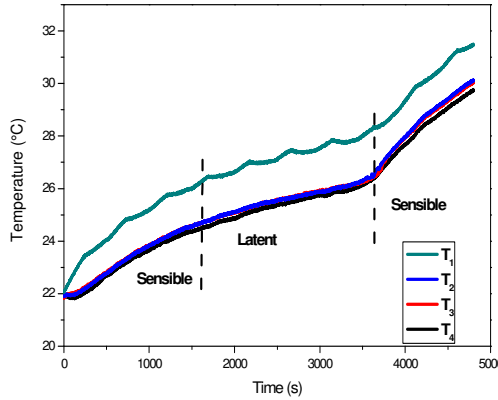


Figure 14: Temperature evolution- RT27, without convection

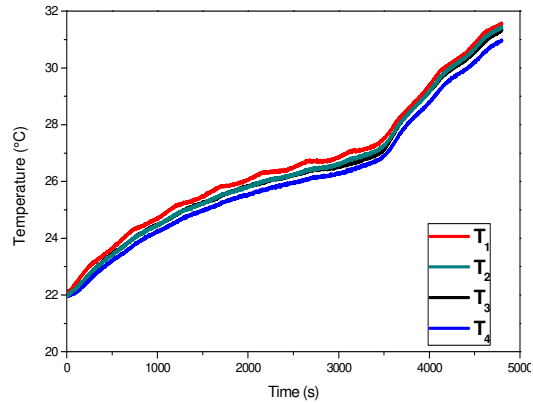


Figure 15: Temperature evolution AF- RT27, without forced convection

246

247 3.2.3. Temperature distribution with forced convection

248 In order to test the effect of convection on the thermal state of the cell, ventilation is activated to
 249 ensure a homogeneous temperature in the climatic chamber (22°C). **Figure 16** presents the time
 250 evolution of the temperature recorded for the pure paraffin RT27. On the one hand a permanent
 251 regime is established after 3 cycles unlike without forced convection. On the other hand, the
 252 temperature difference between T_1 and T_2 increased. The results show that the paraffin is not
 253 completely melted at the end of the test. This can be attributed to heat losses by forced convection.

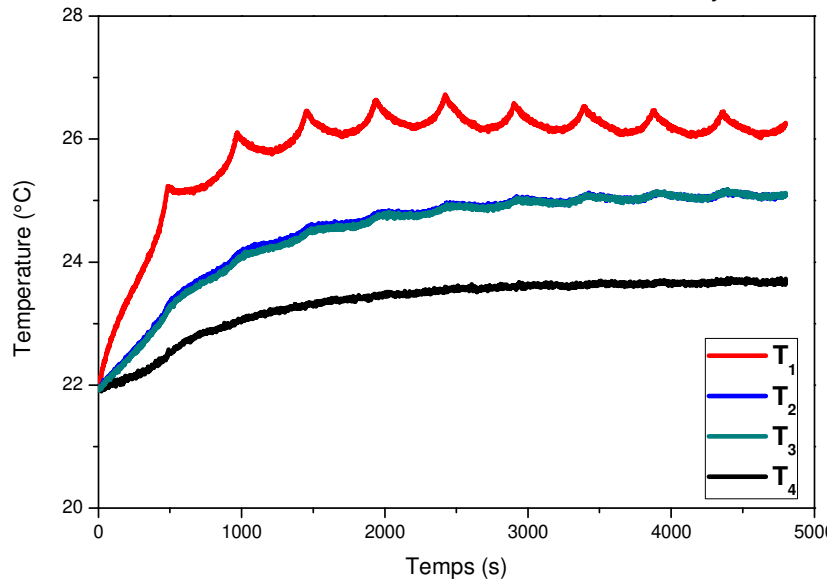


Figure 16: Temperature evolution RT27, forced convection

254

255

256

257 3.2.4. Impact of the addition of metal foam and forced convection

258 **Figure 17** presents the comparison of the cell temperature evolution (T_1) between pure paraffin
 259 RT27 case and paraffin RT27- AF composite case for without forced convection scenario. In this figure

260 it can be seen that the addition of the metal foam reduces the temperature of the cell during the
 261 melting process. Indeed, the addition of a conductive foam intensifies the heat transfer. This has, a
 262 priori, a greater impact in the presence of forced convection. To confirm or deny this, the temporal
 263 temperature of the cell evolution with pure paraffin RT27 was compared to that with paraffin RT27-
 264 AF composite in forced convection scenario, **Figure 18**. The comparison shows an average steady-state
 265 temperature difference of about 1.2°C between the cell temperature with pure RT27 and the Paraffin
 266 RT27- AF composite.

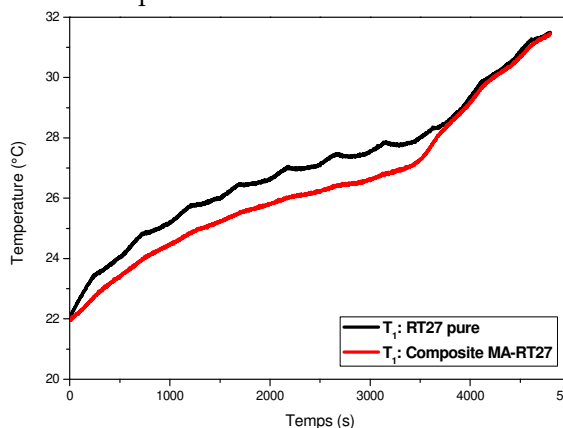


Figure 17: Impact of metal foam on cell temperature, without forced convection scenario

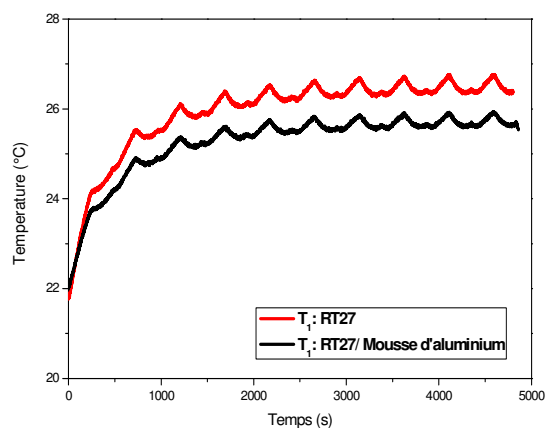


Figure 18: Impact of the addition of a metal foam on the temperature of the cell, with forced convection scenario

267

268 4. Conclusion

269 This paper deals with the study and characterization of thermal phenomena in a Li-ion cell.
 270 Cylindrical 18650 cells were used in this study. This type of cell is the most commonly used in electric
 271 vehicles. An experimental platform has been developed in CERTES Lab to study the thermal behavior
 272 of a Li-ion battery at cell scale. The objective was to propose a new BTMS that guarantees an operating
 273 temperature around the optimal operating temperature of 25°C for 1C charge/discharge cycles. The
 274 following results were obtained:

- 275 • The study of the thermal conductivity of the cell by the Hot-Disk has shown that the axial
 276 thermal conductivity is much more important than the radial one.
- 277 • The results showed that the PCM can absorb the heat generated by the cell in latent form in
 278 solid-liquid phase change. However, its low thermal conductivity limits its performance.
 279 The addition of an aluminum foam allows a more efficient thermal management of the cell.
 280 The results of the temperature measurements revealed that a temperature difference of
 281 about 11°C was recorded on cell surface without the RT27/ Aluminum Foam composite.
- 282 • The proposed BTMS system allowed to keep the temperature of the cell very close to the
 283 optimal operating temperature

284 From the above results, we can conclude that the proposed system can be considered as an
 285 optimized hybrid system which has the potential to be used for Li-ion batteries cooling of electrical
 286 vehicles. Before applying it on the scale of an electric vehicle, this study will be completed by:

- 287 • The study of the thermal performance of the proposed system on the scale of a module and
 288 then on the scale of a pack.
- 289 • Study of the efficiency of the proposed system in the case of severe conditions: fast
 290 discharges (2C, 3C,...)

- 291 • The study of the thermal response of the proposed system with standard cycles: WLTP
- 292 (Worldwide Harmonised Light vehicles Test Procedure).
- 293 • A Durability study of PCM- MF Composites

294

295 **References:**

- 296 [1] Vidadili N, Suleymanov E, Bulut C, Mahmudlu C. Transition to renewable energy and sustainable energy
 297 development in Azerbaijan. *Renewable and Sustainable Energy Reviews* 2017;80:1153–61.
 298 <https://doi.org/10.1016/j.rser.2017.05.168>.
- 299 [2] Liu H, Wei Z, He W, Zhao J. Thermal issues about Li-ion batteries and recent progress in battery thermal
 300 management systems: A review. *Energy Conversion and Management* 2017;150:304–30.
 301 <https://doi.org/10.1016/j.enconman.2017.08.016>.
- 302 [3] Ren Y, Yu Z, Song G. Thermal management of a Li-ion battery pack employing water evaporation.
 303 *Journal of Power Sources* 2017;360:166–71. <https://doi.org/10.1016/j.jpowsour.2017.05.116>.
- 304 [4] Waldmann T, Wilka M, Kasper M, Fleischhammer M, Wohlfahrt-Mehrens M. Temperature dependent
 305 ageing mechanisms in Lithium-ion batteries – A Post-Mortem study. *Journal of Power Sources*
 306 2014;262:129–35. <https://doi.org/10.1016/j.jpowsour.2014.03.112>.
- 307 [5] Ramadass P, Haran B, White R, Popov BN. Capacity fade of Sony 18650 cells cycled at elevated
 308 temperatures: Part II. Capacity fade analysis. *Journal of Power Sources* 2002;112:614–20.
 309 [https://doi.org/10.1016/S0378-7753\(02\)00473-1](https://doi.org/10.1016/S0378-7753(02)00473-1).
- 310 [6] Rizk R, Louahlia H, Gualous H, Schaezel P. Passive Cooling of High Capacity Lithium-Ion batteries.
 311 2018 IEEE International Telecommunications Energy Conference (IN^{TELE}EC) 2018:1–4.
 312 <https://doi.org/10.1109/INTLEC.2018.8612368>.
- 313 [7] Hallaj SA, Selman JR. A Novel Thermal Management System for Electric Vehicle Batteries Using Phase-
 314 Change Material. *J Electrochem Soc* 2000;147:3231. <https://doi.org/10.1149/1.1393888>.
- 315 [8] Wu S, Yan T, Kuai Z, Pan W. Thermal conductivity enhancement on phase change materials for thermal
 316 energy storage: A review. *Energy Storage Materials* 2020;25:251–95.
 317 <https://doi.org/10.1016/j.ensm.2019.10.010>.
- 318 [9] Biwole PH, Groulx D, Souayfane F, Chiu T. Influence of fin size and distribution on solid-liquid phase
 319 change in a rectangular enclosure. *International Journal of Thermal Sciences* 2018;124:433–46.
 320 <https://doi.org/10.1016/j.ijthermalsci.2017.10.038>.
- 321 [10] Conductivity particles dispersed organic and inorganic phase change materials for solar energy storage—an
 322 exergy based comparative evaluation. *Energy Procedia* 2012;14:643–8.
 323 <https://doi.org/10.1016/j.egypro.2011.12.989>.
- 324 [11] Ren Q, Guo P, Zhu J. Thermal management of electronic devices using pin-fin based cascade
 325 microencapsulated PCM/expanded graphite composite. *International Journal of Heat and Mass Transfer*
 326 2020;149:119199. <https://doi.org/10.1016/j.ijheatmasstransfer.2019.119199>.
- 327 [12] EL IDI MM, Karkri M. Méthode inverse pour la détermination expérimentale des propriétés
 328 thermophysiques des matériaux à changement de phase. *Congrès Français de Thermique, SFT 2018, PAU,*
 329 *France: 2018.*
- 330 [13] Boussaba L, Foufa A, Makhlof S, Lefebvre G, Royon L. Elaboration and properties of a composite bio-
 331 based PCM for an application in building envelopes. *Construction and Building Materials* 2018;185:156–
 332 65. <https://doi.org/10.1016/j.conbuildmat.2018.07.098>.
- 333 [14] Sarani I, Payan S, Nada SA, Payan A. Numerical investigation of an innovative discontinuous distribution
 334 of fins for solidification rate enhancement in PCM with and without nanoparticles. *Applied Thermal*
 335 *Engineering* 2020;176:115017. <https://doi.org/10.1016/j.applthermaleng.2020.115017>.
- 336 [15] Dinesh BVS, Bhattacharya A. Comparison of energy absorption characteristics of PCM-metal foam
 337 systems with different pore size distributions. *Journal of Energy Storage* 2020;28:101190.
 338 <https://doi.org/10.1016/j.est.2019.101190>.
- 339 [16] El idi MM, Karkri M, Kraiem M. Preparation and effective thermal conductivity of a Paraffin/ Metal Foam
 340 composite. *Journal of Energy Storage* 2020:102077. <https://doi.org/10.1016/j.est.2020.102077>.
- 341 [17] Moussa EL IDI M, Karkri M. Heating and cooling conditions effects on the kinetic of phase change of
 342 PCM embedded in metal foam. *Case Studies in Thermal Engineering* 2020:100716.
 343 <https://doi.org/10.1016/j.csite.2020.100716>.
- 344 [18] Mohamed Moussa EI, Karkri M. A numerical investigation of the effects of metal foam characteristics and
 345 heating/cooling conditions on the phase change kinetic of phase change materials embedded in metal
 346 foam. *Journal of Energy Storage* 2019;26:100985. <https://doi.org/10.1016/j.est.2019.100985>.
- 347 [19] EL IDI MM, Karkri M. Etude numérique de stockage d'énergie thermique dans un composite : mousses
 348 métalliques/matériaux à changement de phase. *Congrès Français de Thermique SFT 2019, Nantes, France:*
 349 *2019.*

- 350 [20] EL IDI MM, KARKRI M. Melting and solidification behavior of PCM embedded in metal foam.
351 COMSOL CONFERENCE 2020 EUROPE, Grenoble, France: 2020.
- 352 [21] Tauseef-ur-Rehman, Ali HM, Janjua MM, Sajjad U, Yan W-M. A critical review on heat transfer
353 augmentation of phase change materials embedded with porous materials/foams. *International Journal of*
354 *Heat and Mass Transfer* 2019;135:649–73. <https://doi.org/10.1016/j.ijheatmasstransfer.2019.02.001>.
- 355 [22] Ashby MF, Evans AG, Fleck NA, Gibson LJ, Hutchinson JW, Wadley HNG, editors. Chapter 4 -
356 Properties of metal foams. *Metal Foams*, Burlington: Butterworth-Heinemann; 2000, p. 40–54.
357 <https://doi.org/10.1016/B978-075067219-1/50006-4>.
- 358 [23] Weng J, He Y, Ouyang D, Yang X, Zhang G, Wang J. Thermal performance of PCM and branch-
359 structured fins for cylindrical power battery in a high-temperature environment. *Energy Conversion and*
360 *Management* 2019;200:112106. <https://doi.org/10.1016/j.enconman.2019.112106>.
- 361 [24] Ping P, Peng R, Kong D, Chen G, Wen J. Investigation on thermal management performance of PCM-fin
362 structure for Li-ion battery module in high-temperature environment. *Energy Conversion and Management*
363 2018;176:131–46. <https://doi.org/10.1016/j.enconman.2018.09.025>.
- 364 [25] Ouyang D, Weng J, Hu J, Liu J, Chen M, Huang Q, et al. Effect of High Temperature Circumstance on
365 Lithium-Ion Battery and the Application of Phase Change Material. *J Electrochem Soc* 2019;166:A559.
366 <https://doi.org/10.1149/2.0441904jes>.
- 367 [26] Ling Z, Chen J, Fang X, Zhang Z, Xu T, Gao X, et al. Experimental and numerical investigation of the
368 application of phase change materials in a simulative power batteries thermal management system.
369 *Applied Energy* 2014;121:104–13. <https://doi.org/10.1016/j.apenergy.2014.01.075>.
- 370 [27] Hussain A, Abidi IH, Tso CY, Chan KC, Luo Z, Chao CYH. Thermal management of lithium ion batteries
371 using graphene coated nickel foam saturated with phase change materials. *International Journal of*
372 *Thermal Sciences* 2018;124:23–35. <https://doi.org/10.1016/j.ijthermalsci.2017.09.019>.
- 373 [28] Li WQ, Qu ZG, He YL, Tao YB. Experimental study of a passive thermal management system for high-
374 powered lithium ion batteries using porous metal foam saturated with phase change materials. *Journal of*
375 *Power Sources* 2014;255:9–15. <https://doi.org/10.1016/j.jpowsour.2014.01.006>.
- 376 [29] Bamdezh MA, Molaeimanesh GR, Zanganeh S. Role of foam anisotropy used in the phase-change
377 composite material for the hybrid thermal management system of lithium-ion battery. *Journal of Energy*
378 *Storage* 2020;32:101778. <https://doi.org/10.1016/j.est.2020.101778>.
- 379 [30] Bamdezh MA, Molaeimanesh GR. Impact of system structure on the performance of a hybrid thermal
380 management system for a Li-ion battery module. *Journal of Power Sources* 2020;457:227993.
381 <https://doi.org/10.1016/j.jpowsour.2020.227993>.
- 382 [31] Mehrabi-Kermani M, Houshfar E, Ashjaee M. A novel hybrid thermal management for Li-ion batteries
383 using phase change materials embedded in copper foams combined with forced-air convection.
384 *International Journal of Thermal Sciences* 2019;141:47–61.
385 <https://doi.org/10.1016/j.ijthermalsci.2019.03.026>.
- 386 [32] Zhang H, Wu X, Wu Q, Xu S. Experimental investigation of thermal performance of large-sized battery
387 module using hybrid PCM and bottom liquid cooling configuration. *Applied Thermal Engineering*
388 2019;159:113968. <https://doi.org/10.1016/j.applthermaleng.2019.113968>.
- 389 [33] Hekmat S, Molaeimanesh GR. Hybrid thermal management of a Li-ion battery module with phase change
390 material and cooling water pipes: An experimental investigation. *Applied Thermal Engineering*
391 2020;166:114759. <https://doi.org/10.1016/j.applthermaleng.2019.114759>.
- 392 [34] Mashayekhi M, Houshfar E, Ashjaee M. Development of hybrid cooling method with PCM and Al₂O₃
393 nanofluid in aluminium minichannels using heat source model of Li-ion batteries. *Applied Thermal*
394 *Engineering* 2020;178:115543. <https://doi.org/10.1016/j.applthermaleng.2020.115543>.
- 395 [35] Lv Y, Liu G, Zhang G, Yang X. A novel thermal management structure using serpentine phase change
396 material coupled with forced air convection for cylindrical battery modules. *Journal of Power Sources*
397 2020;468:228398. <https://doi.org/10.1016/j.jpowsour.2020.228398>.
- 398 [36] Pesaran A, Keyser M, Kim GH, Santhanagopalan S, Smith K. Tools for Designing Thermal Management
399 of Batteries in Electric Drive Vehicles. National Renewable Energy Lab. (NREL), Golden, CO (United
400 States); 2013. <https://doi.org/10.2172/1064502>.
- 401 [37] Kraiem M, Karkri M, Nasrallah SB, Sobolciak P, Fois M, Alnuaimi NA. Thermophysical Characterization
402 and Numerical Investigation of Three Paraffin Waxes as Latent Heat Storage Materials 2019.
403 <https://doi.org/10.20944/preprints201903.0034.v1>.
- 404 [38] El Idi MM, Karkri M, Abdou Tankari M. A passive thermal management system of Li-ion batteries using
405 PCM composites: Experimental and numerical investigations. *International Journal of Heat and Mass*
406 *Transfer* 2021;169:120894. <https://doi.org/10.1016/j.ijheatmasstransfer.2020.120894>.
- 407 [39] Gustafsson SE. Transient plane source techniques for thermal conductivity and thermal diffusivity
408 measurements of solid materials. *Review of Scientific Instruments* 1991;62:797–804.
409 <https://doi.org/10.1063/1.1142087>.

410 [40] Log T, Gustafsson SE. Transient plane source (TPS) technique for measuring thermal transport properties
411 of building materials. *Fire and Materials* 1995;19:43–9. <https://doi.org/10.1002/fam.810190107>.

412 [41] Hot Disk | Anisotropy Thermal Conductivity Tests of Batteries. Hot Disk n.d.
413 <https://www.hotdiskinstruments.com/applications/anisotropy-thermal-conductivity-tests-of-batteries/>
414 (accessed August 7, 2020).

415 [42] Wang Z, Zhang H, Xia X. Experimental investigation on the thermal behavior of cylindrical battery with
416 composite paraffin and fin structure. *International Journal of Heat and Mass Transfer* 2017;109:958–70.
417 <https://doi.org/10.1016/j.ijheatmasstransfer.2017.02.057>.

418 [43] Weng J, Ouyang D, Yang X, Chen M, Zhang G, Wang J. Optimization of the internal fin in a phase-
419 change-material module for battery thermal management. *Applied Thermal Engineering*
420 2020;167:114698. <https://doi.org/10.1016/j.applthermaleng.2019.114698>.

421 [44] Choudhari VG, Dhoble AS, Panchal S. Numerical analysis of different fin structures in phase change
422 material module for battery thermal management system and its optimization. *International Journal of*
423 *Heat and Mass Transfer* 2020;163:120434. <https://doi.org/10.1016/j.ijheatmasstransfer.2020.120434>.

424